DOI https://doi.org/10.30525/978-9934-26-329-3-9

ELECTROCHEMICAL DEPOSITION OF COMPLEX CHROMOXIDE COMPOSITES ON STAINLESS STEEL

Shtefan V. V., Kanunnikova N. O., Dubrovskyi V. S.

INTRODUCTION

The development of modern science and technology requires the creation of the latest composite materials that will work successfully and have an appropriate level of their functional properties under the influence of aggressive environments. Thus, at present, solving the issues of protection of materials and structures of nuclear reactors from various types of corrosion destruction is a priority task, which necessitates the development of new means of protection of corrosion-resistant materials[1]. One of the effective methods of forming coatings with the necessary set of properties on the surface of metals is the electrochemical method[2].

With cathodic polarization, non-porous, dense oxide composites are formed on the surfaces of metals, which allow not only to ensure safe operation, but also to significantly reduce the costs of repair and restoration after breakdowns, destruction of products and complex technical systems under the influence of climatic factors[3]. The composition and properties of oxide composites are determined by the nature of the metal and electrolyte, as well as depend on the conditions of their production, which makes it possible to control the process[4].

Watson S.W. proposed a method of depositing a chromium coating on stainless steel for corrosion protection. By adding to the electrolyte to obtain a coating of particles of solid compounds, such as diamonds, WC and SiC, which also provide better not only protection against metal corrosion, but also

---

[1] Haq I.U., Akhtar K., Khan Tahir.I., Ali Shah A. Electrodeposition of Ni–Fe_2O_3 nanocomposite coating on steel. Surface and Coatings Technology. 2013. V. 235. P. 691-698. https://doi.org/10.1016/j.surfcoat.2013.08.048.

[2] Georgieva J., Armyanov S., Valova E., Poulios I., Sotiropoulos S. Preparation and photoelectrochemical characterisation of electrosynthesised titanium dioxide deposits on stainless steel substrates. Electrochimica Acta. 2006. V. 51. P. 2076-2087. https://doi.org/10.1016/j.electacta.2005.07.017.

[3] Junqueira R.M.R., Manfridini A.P. de Andrade, Loureiro C.R. de Oliveira et all. Morphological, chemical and mechanical characteristics of an anodic coating on stainless steel. Surface Engineering. 2013. V. 29. P. 379-383. https://doi.org/10.1179/1743294413Y.0000000126.

[4] Klimas V., Pakštas V., Vrublevsky I., Chernyakova K., Jagminas A. Fabrication and Characterization of Anodic Films onto the Type-304 Stainless Steel in Glycerol Electrolyte. J. Phys. Chem. C. 2013. V. 117. P. 20730-20737. https://doi.org/10.1021/jp407028u.

resistance to abrasive wear[5]. In addition, electrolytic deposited chromoxide composites can be used to increase the service life of metal surfaces that act as contact groups. Also, particles of anti-friction materials such as graphite, MoS_2 and PTFE in these coatings reduce friction between metal surfaces[6]. In addition, the use of a dispersed MoS_2 phase leads to a change in the microstructure of the matrix metal itself by grinding the mosaic blocks. These hard materials are too brittle and have to low adhesion to metal surfaces to be used directly as a coating. Thus, the metal matrix is used to hold the particles together and promote good adhesion to the metal surface of the part[7].

The effect of technological parameters on the deposition of chromium-corundum coatings from the universal chromium plating electrolyte is also considered in scientific works. It is shown that in the electrolyte and in the suspension based on it, over the entire range of technological parameters, chromium crystallizes into a cubic modification[8]. The density and temperature regime of electrolysis equally affect the amount of microvoltage of chromium deposits that are formed in a purely universal electrolyte and in the electrolyte of composite chromium plating[9,10]. With an increase in the temperature of the electrolyte from about 40 to 50°C, a tendency to decrease microvoltages in the coatings was observed. An increase in the density of the cathode current, on the contrary, leads to an increase in microvoltages. The addition of finely dispersed particles of corundum to the electrolyte with their limited

---

[5] Arevalo Marulanda J.L., Pérez Trujillo F.J., Castañeda S.I. Aluminum-silicon coatings on austenitic stainless steel (AISI 304 and 317) deposited by chemical vapor deposition in a fluidized bed: Recubrimientos de aluminio-silicio sobre acero inoxidable austenítico AISI 304 Y 317 por deposición química de vapor en lecho fluidizado. Ing. Inv. 2014. V. 34. P. 5-10. https://doi.org/10.15446/ing.investig.v34n2.41249.

[6] Shtefan V.V., Smyrnov O.O., Bezhenko A.O., Epifanova A.S., Kanunnikova N.O., Metenkanych M.M., Knyazev S.A. Corrosion of Cobalt-Molybdenum Alloys in Chloride Solutions. Mater Sci. 2019. V. 54 P. 512-518. https://doi.org/10.1007/s11003-019-00225-y.

[7] Ingle A.V., Raja V.S., Mishra P. et al, Effect of Mo Addition on the Corrosion Behavior of Al-40Cr-xMo Coatings on Type 316L Stainless Steel. Metall Mater Trans A. 2020. V. 51. P. 1933-1944. https://doi.org/10.1007/s11661-020-05628-0

[8] Bellezze T., Roventi G., Quaranta A., Fratesi R. Improvement of pitting corrosion resistance of AISI 444 stainless steel to make it a possible substitute for AISI 304L and 316L in hot natural waters: Improvement of pitting corrosion resistance of stainless steel. Materials and Corrosion. 2008. V. 59. P. 727-731. https://doi.org/10.1002/maco.200804112.

[9] Shen Y.Z., Guo X.Z., Lin Y.BTao., J. Al_2O_3 coatings fabricated on stainless steel/aluminium composites by microarc oxidation. Surface Engineering. 2014. V. 30. P. 735-740. https://doi.org/10.1179/1743294414Y.0000000300.

[10] Šípová M., Marušáková D., Aparicio C., Procházka J., Halodová P. A study on the corrosion behaviour of stainless steel 08Cr18Ni10Ti in supercritical water. Corrosion Science. 2023.Vol. 211. P. 110853. https://doi.org/10.1016/j.corsci.2022.110853

interference in the chromium matrix (0.45-0.78 wt%) has practically no effect on the change in the value of microvoltages (1000-1400)[11].

The purpose of this work is to establish the kinetic patterns of formation and electrochemical deposition of chromoxide composites with high protective and electrical insulating properties.

1. Kinetic regularities of the formation of chromoxide composites

The study of the laws of the kinetics of the formation of chromoxide composites on stainless steel is important, as they have practical significance in such technologies as surface treatment of materials and electrochemical protection of metals and alloys from corrosion[12,13]. The lack of reliable information on the kinetics and mechanisms of the formation of metal oxide compositions of highly alloyed stainless steels is a serious omission, since they should be the basis for predicting the properties of coatings and developing anti-corrosion protection[14]. Modification of chromoxide composites in order to increase the protective and dielectric properties of composite materials requires a preliminary study of the influence of titanium and aluminum oxides on the kinetic patterns of the formation of chromoxide composites[15].

The study of the kinetics of the formation of chromoxide composites was carried out in a three-electrode electrochemical cell using an IPC-Pro potentiostat-galvanostat. AISI 304 steel samples without and with chromoxide composites with a surface area of 1 cm^2 were used as the working electrode. The potential of the studied steel electrode was measured relative to the potential of the EVL-1M1 silver chloride electrode. The auxiliary electrode is platinum. The potential sweep rate is 2 mV/s. The experiments were carried out under conditions of natural convection at an electrolyte temperature of

---

[11] Rajakaruna R. M. P. I., Ariyarathna, I. R. Functionalized metal-based nanoelectrocatalysts for water splitting. Handbook of Functionalized Nanomaterials for Industrial Applications. 2020. P. 83–109. https://doi.org/10.1016/b978-0-12-816787-8.00004-1

[12] Huang L., Yao B., Sun J. et all. Highly conductive and flexible molybdenum oxide nanopaper for high volumetric supercapacitor electrode. J. Mater. Chem. A. 2017. V. 5. P. 2897-2903. https://doi.org/10.1039/C6TA10433A.

[13] Shtefan V.V., Kanunnikova N.O., Goncharenko T.Ye. Analysis of the Structure and Anticorrosion Properties of Oxide Coatings on AISI 304 Steel. Mater Sci. 2021. V. 57. P. 248-255. https://doi.org/10.1007/s11003-021-00539-w.

[14] Geng S., Qi S., Zhao Q., Zhu S., Wang F. Electroplated Ni–Fe_2O_3 composite coating for solid oxide fuel cell interconnect application. International Journal of Hydrogen Energy. 2012. V. 37. P. 10850-10856. https://doi.org/10.1016/j.ijhydene.2012.04.043.

[15] Shtefan V.V., Balamut N.S., Kanunnikova N.A. et all. Electrodeposition of chromoxide coatings from electrolytes modified with $SiO_2{\cdot}nH_2O$, Problems of Atomic Science and Technology(PAST), 2022. V. 140. P. 131-136. https://doi.org/10.46813/2022-140-131.

25ºC[16]. At least five polarization curves per sample were recorded to check the reproducibility of the measurements.

The influence of TiO_2 on the kinetic regularities of the formation of composites. The nature of the dependence of AISI 304 obtained in a chromium-containing solution without the addition of TiO_2 (Fig. 1) is similar to that given in the total polarization curve of chromium electrodeposition. As can be seen, the speed of the process initially increases strongly (section ab), which indicates an active state of the surface, but when the potential is further increased, it gradually decreases (section bc) and increases upon reaching a potential of -700 mV (section cd) [17].

At the potentials corresponding to individual sections of the cathodic polarization dependence No. 1, the following electrochemical reactions take place:

1) In the section ab there is an incomplete reduction of Cr^{6+} до Cr^{3+} according to the equation:

$CrO_4^{2-} + 4H_2O + 3e \rightarrow Cr^{3+} + 8OH^-$ (a)

2) In the section ab, in parallel with reaction (a), hydrogen is released:

$3H_3O^+ + 2e \rightarrow H_2 + 2H_2O$ (б)

3) In the cd region, three reactions occur simultaneously: (a), (b) and the reduction of Cr^{6+}, Cr^{3+} to Cr[18,19].

When non-conductive particles of titanium dioxide are introduced into the composition of the chromium-containing electrolyte, the potentials for the formation of chromoxide composites shift to the electronegative side, which is associated with the shielding of part of the active surface of the cathode by non-conductive particles.

---

[16] Taveira L.V., Montemor M.F., Belo M. Da Cunha. Influence of incorporated Mo and Nb on the Mott–Schottky behaviour of anodic films formed on AISI 304L. Corrosion Science. 2010. V. 52. P. 2813-2818. https://doi.org/10.1016/j.corsci.2010.04.021.

[17] Shtefan V., Kanunnikova N., Balamut N. Anodic oxidation of AISI 304 steel in acidic solutions. Proceedings of Odessa Polytechnic University. 2018. V 56. № 3. P. 89-94. https://doi.org/10.15276/opu.3.56.2018.09

[18] Maier B., Frankel G. S. Pitting Corrosion of Bare Stainless Steel 304 under Chloride Solution Droplets. Journal of The Electrochemical Society. 2010. V. 157(10). P. 302. https://doi.org/10.1149/1.3467850

[19] Shtefan V., Kanunnikova N., Bulhakova A. et al. Structural and Phase Analysis of Composites Based on TiO_2. Surf. Engin. Appl.Electrochem. V. 58. P. 598-603 https://doi.org/10.3103/S1068375522060138.

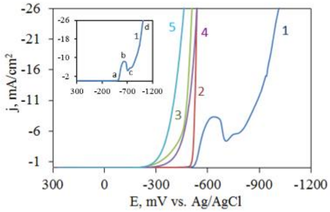

Fig. 1. Cathodic polarization dependences of AISI 304 steel. Electrolyte, g/L: CrO_3 – 250, H_3BO_3 – 20, $NaNO_3$ – 5, $Ba(OH)_2$ – 2, TiO_2 – 0 (1); 30 (2); 50 (3); 70 (4); 100 (5)

Since, during the deposition of chromium, a combined reaction of hydrogen evolution occurs, in order to understand the kinetics and mechanism of the formation of composites, it is necessary to consider the dependence of the polarization current density on the hydrogen evolution overvoltage[20,21].

Graphs of the dependence η – lgj may have a clear linear character (Fig. 2).

The calculated Tafel constants *a*, *b* and products of transfer coefficients by the number of electrons *αz* are presented in the Table 1. As can be seen from the obtained data, with an increase in the concentration of TiO_2 in the composition of chromium-containing electrolytes, the value of the constant *a* decrease, which indicates an increase in the rate of the hydrogen electrolysis reaction. At the same time, the constant *b* changes when the concentration of TiO_2 varies.

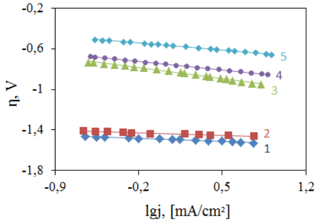

Fig. 2. Tafel dependencies on AISI 304 steel with chromoxide composites obtained from chromium-containing solutions (show Table 1) with the addition of TiO_2, g/L: 0 (1); 30 (2); 50 (3); 70 (4); 100 (5)

---

[20] Пат. на кор. мод. № 147835 Україна, МПК C25D 11/34. Спосіб формування захисних оксидних покриттів на нержавіючій сталі / Штефан В.В., Смирнова О.Ю., Кануннікова Н.О. Баламут Н.С.; заявник та власник патенту НТУ «ХПІ». – № u202008156; заявл. 21.12.2020; опубл. 16.06.2021, бюл. № 24. https://base.uipv.org/searchINV/search.php?action=viewdetails&IdClaim=276584

[21] Zuyok V., Rud R., Shtefan V. et all. Assessment of the corrosion resistance of the main alternative materials for light water reactors tolerant fuel rod cladding. Problems of Atomic Science and Technology. 2022. V. 140(4). P. 89-96. https://doi.org/10.46813/2022-140-089

Table 1

Kinetic parameters of cathodic formation of $Cr\cdot CrO_x\cdot TiO_y$ composites

The composition of the electrolyte, g/L					Kinetic parameters		
CrO_3	H_3BO_3	$NaNO_3$	$Ba(OH)_2$	TiO_2	– *a*, B	– *b*, B	*αz*
250	20	5	2	-	1,49	0,03	1,81
250	20	5	2	30	1,43	0,03	1,81
250	20	5	2	50	0,81	0,12	0,45
250	20	5	2	70	0,74	0,12	0,45
250	20	5	2	100	0,56	0,12	0,61

The thus obtained value of the constant *b*, which was 0.03 V, for chromium-containing electrolytes without and with the addition of 30 g/L TiO_2 testifies against the slowing down of a purely electrochemical stage and is better consistent with the theory of slowed down recombination of adsorbed hydrogen atoms. When the concentration of TiO_2 is increased to 50-100 g/L, the constant b becomes 0.12 V and indicates that the limiting stage of the electrochemical process of hydrogen evolution is the stage of delayed discharge with subsequent electrochemical desorption of hydrogen atoms. From the obtained *αz* values, it can be concluded that the cathodic discharge process occurs more easily in chromium-containing electrolytes without and with the addition of 30 g/L TiO_2, i.e., the formation of chromoxide composites will be faster.

The influence of Al_2O_3 on the kinetic regularities of the formation of composites. When Al_2O_3 particles are introduced into the composition of chromium-containing electrolytes, the character of the cathode polarization dependence of AISI 304 steel changes (Fig. 3) and the potentials for the formation of chromoxide composites shift to the electronegative side, which indicates inhibition of cathodic reactions due to shielding of the working surface of the steel with non-conductive particles[22,].

---

[22] Mansfeld F., Kendig, M. Technical Note:Concerning the Choice of Scan Rate in Polarization Measurements. Corrosion. 1981. V. 37(9). P. 545-546. https://doi.org/10.5006/1.3580804

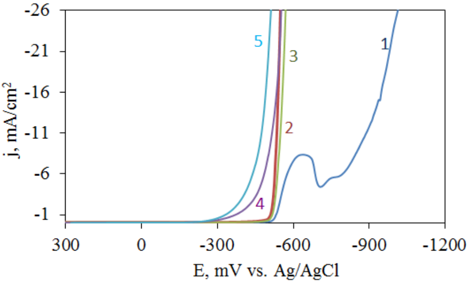

Fig. 3. Cathodic polarization dependences of AISI 304 steel. Electrolyte, g/L: CrO_3 – 250, H_3BO_3 – 20, $NaNO_3$ – 5, $Ba(OH)_2$ – 2, Al_2O_3 – 0 (1); 30 (2); 50 (3); 70 (4); 100 (5).

The resulting cathode polarization dependencies in Tafel coordinates are linear in nature (Fig. 4). The calculated kinetic parameters (*a, b, αz*) of the cathodic formation of chromoxide composites $Cr \cdot CrO_x \cdot Al_xO_y$ are shown in the Table 2.

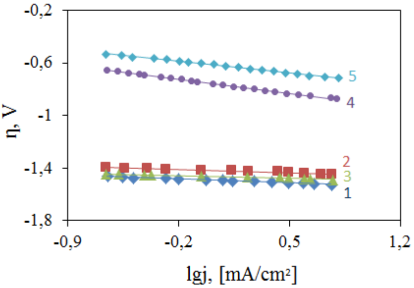

Fig. 4. Tafel dependencies on AISI 304 steel with chromoxide composites obtained from chromium-containing solutions (show Table 2) with the addition of Al_2O_3, g/L: 0 (1); 30 (2); 50 (3); 70 (4); 100 (5).

The analysis of the obtained data shows that an increase in the concentration of Al_2O_3 in the composition of chromium-containing electrolytes decreases the value of the constant a, and this, in turn, indicates an increase in the rate of the hydrogen evolution reaction[23].

---

[23] Shtefan V.V., Kanunnikova N.A. Oxidation of AISI 304 Steel in Al– and Ti-Containing Solutions. Prot Met Phys Chem Surf. 2020. V. 56. P. 379-384. https://doi.org/10.1134/S2070205120020239.

Table 2

Kinetic parameters of cathodic formation of $Cr\cdot CrO_x\cdot Al_xO_y$ composites

The composition of the electrolyte, g/L					Kinetic parameters		
CrO_3	H_3BO_3	$NaNO_3$	$Ba(OH)_2$	Al_2O_3	– *a*, B	– *b*, B	*αz*
250	20	5	2	-	1,49	0,03	1,81
250	20	5	2	30	1,45	0,03	1,81
250	20	5	2	50	1,40	0,03	0,81
250	20	5	2	70	0,74	0,12	0,45
250	20	5	2	100	0,61	0,12	0,45

As follows from the calculated values of constant b for electrolytes given in Table 2, when the Al_2O_3 concentration is increased to 70-100 g/L, the cathodic hydrogen release mechanism changes, which is confirmed by the *αz* values. Thus, with the introduction of particles with a concentration of 30-50 g/L, the value *b* = 0,03 V, which indicates the release of hydrogen according to the theory of delayed recombination, and at 70-100 g/L, *b* = 0,12 V and is determined by the delayed discharge stage with the following electrochemical desorption of hydrogen atoms.

2. Electrochemical formation of chromoxide composites

This section is devoted to the substantiation of the components and modes of electrochemical formation and to the study of the structure, elemental and phase composition of the obtained chromoxide composites on the basis of studies of the kinetic laws of the formation of composites.

For the formation of chromoxide composites, samples of AISI 304 steel with a surface area of 4 cm^2 were used, which were previously activated at a temperature of 18-25°C for 30 minutes in a solution of 5% sulfuric acid at a cathodic current of -250 mA to remove the natural oxide film. It was found that the activation of the steel surface also contributes to a more durable adhesion of the coating to the base[24].

Electrochemical formation was carried out in the galvanostatic mode at a current density of 70 A/dm^2 for 50 minutes in a basic electrolyte with the composition, g/L: CrO_3 – 250, H_3BO_3 – 20, $Ba(OH)_2$ – 2, $NaNO_3$ – 5 with the addition of TiO_2 or Al_2O_3 concentration 30-100. The process was carried out in a two-electrode cell with a working volume of 200 ml with a continuous stirring system. A plate made of AISI 304 steel with a surface area of 4 cm^2

---

[24] Shtefan V., Kanunnikova N., Pilipenko A., Pancheva H. Corrosion Behavior of AISI 304 Steel in Acid Solutions. Materials Today: Proceedings. 2019. V. 6. P. 150-157. https://doi.org/10.1016/j.matpr.2018.10.088.

was used as a cathode, and platinum served as a counter electrode. The temperature of the electrolyte is 18-25°C[25].

The obtained chromoxide composites are black in colour, uniform, continuous and well bonded to the base. Modifications with aluminum and titanium oxides do not affect the colour of composites and electrolysis parameters. Therefore, as it was found out, a decrease in the current density to 30 A/dm^2 leads to the formation of very thin films and the colour of the coating becomes shiny black, and when it is increased to 80 A/dm^2, black rough coatings are deposited («burning»).

It was established that an increase in the temperature of the electrolyte leads to the formation of a loose composite that is poorly bonded to the steel. In order to intensify the process of forming high-quality chromoxide composites, mixing was used. For the formation of higher-quality composites on stainless steel, it is necessary to form for at least 40 minutes. The regularities of obtaining chromoxide composites are similar both from basic chromium-containing and from titanium– and aluminum-containing electrolytes.

Morphology, SEM. The surface morphology and elemental composition of the obtained composites were studied using a ZEISS EVO 40XVP scanning electron microscope (SEM) equipped with an INCA Energy 350 microanalysis system manufactured by Carl Zeiss (Germany) and Oxford Instruments (England). The SMARTSEM software environment is used to process the received images[26].

The surfaces of the composites formed in electrolytes with the addition of TiO_2 (Figure 5, 2), Al_2O_3 (Figure 5, 3) differed in the width and number of cracks from the chromium-containing composite (deposited in the electrolyte without introducing TiO_2, Al_2O_3 particles (Figure 5, 1)).

As can be seen from Figs. 5 and 6, the surface of the $Cr\cdot CrO_x$, $Cr\cdot CrO_x\cdot MO_{y(z)}$ composites is uneven and protrusions in the form of pyramids and petals are observed throughout the surface. It should be noted that the obtained structure of chromoxide composites is more continuous than the structure obtained by the authors.

Chromoxide composites do not have a distinct texture, as shown in Fig. 5. Crystals form on the surface in the form of petals, which have different orientations.

---

[25] Slemnik M., Milošev I. An impedance study of two types of stainless steel in Ringer physiological solution containing complexing agents. Journal of Materials Science: Materials in Medicine. 2006. V. 17(10). P. 911-918. https://doi.org/10.1007/s10856-006-0180-0

[26] Shtefan V.V., Kanunnikova N.A. Electrochemical formation of molybdenum-coating anode oxide coatings on AISI 304 steel. Promising Materials and Processes in Applied Electrochemistry: Monograph / Editor-in-chief V.S. Barsukov. Kyiv: KNUTD. 2019. P. 97-110.

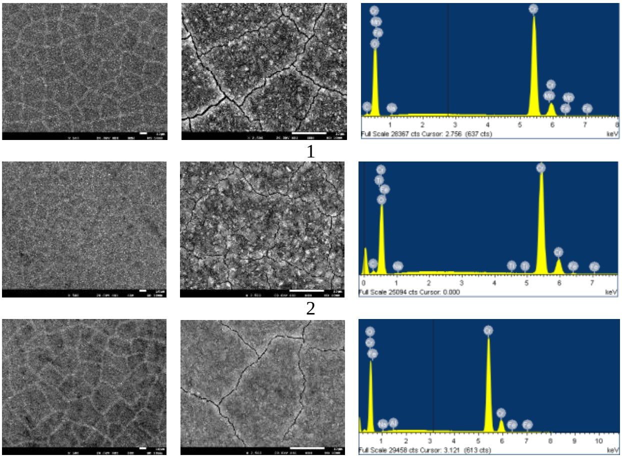

1

2

3

Fig. 5. SEM images and EDX – surface spectra of composites: Cr·CrO$_x$ (1), Cr·CrO$_x$·TiO$_y$ (2), Cr·CrO$_x$·Al$_x$O$_y$ (3)

Formed chromoxide composites contain such elements as oxygen, chromium, titanium and aluminum (Table 3). Since the composites have a large amount of oxygen in their composition, it can be concluded that the obtained chromoxide composites contain enough oxygen-containing compounds with chromium. The possibility of incorporating dispersed particles from electrolyte suspensions into the composition of composite materials during electrochemical forming on the surface of chrome-nickel steels has been noted and is gaining popularity recently.

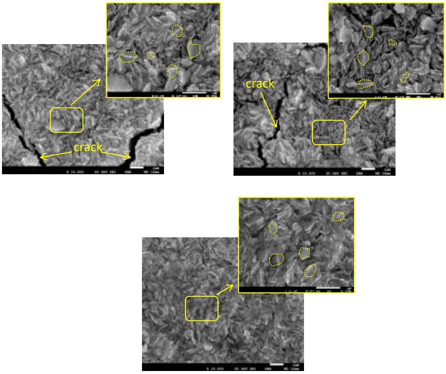

Fig. 6. SEM images of composites: Cr·CrO$_x$ (1), Cr·CrO$_x$·TiO$_y$ (2), Cr·CrO$_x$·Al$_x$O$_y$ (3)

X-ray Phase Analysis. The phase composition of the obtained composites was studied on a DRON-3.0 X-ray diffractometer (CuKα radiation) and phases were identified using the ASTM file[27,28].

Analysis of radiographs of AISI 304/$Cr\cdot CrO_x\cdot MO_{y(z)}$ (M = Ti, Al) showed that all chromoxide composites consist of chromium and iron oxides (Table 3), and $Cr\cdot CrO_x\cdot TiO_y$ and $Cr\cdot CrO_x\cdot Al_xO_y$ composites also contain titanium oxides and aluminum oxides. Therefore, it can be assumed that the presence of these compounds in the corresponding phases in the coating gives the composites high anti-corrosion and insulating properties[29]. Varying the concentration of valve metal oxides does not significantly affect the phase composition, and it should be noted that the structure of all formed chromoxide composites is crystalline. The presence of the $Fe_{0,98}O$ phase can be explained by the fact that during the analysis of the surface the beam reached the substrate.

Table 3

Elemental and phase composition of chromoxide composites on AISI 304 steel

Composite	Elemental composition, mass.%	Phase composition
$Cr\cdot CrO_x$	O – 32,02; Cr – 67,05, Na – 0,22; Mn – 0,30, Fe – 0,51	FeO, $Fe_{0,98}O$, $(Cr, Fe)_2O_3$, Cr_3O_4, β–Fe_2O_3, C_2FeO_4
$Cr\cdot CrO_x\cdot TiO_y$	O – 30,00; Cr – 65,22; Ti – 5,49, Na – 0,19; Fe – 0,56	$Fe_{0,98}O$, CrO_3, TiO_2
$Cr\cdot CrO_x\cdot Al_xO_y$	O – 30,23; Cr – 62,79; Al – 7,37, Na – 0,37; Fe – 0,49	FeO, $Fe_{0,98}O$, $(Cr, Fe)_2O_3$, Cr_3O_4, β–Fe_2O_3, CrO_3, C_2FeO_4, Al_2O_3

---

[27] Li Z.Y., Cai Z.B., Cui X.J. et al., Influence of nanoparticle additions on structure and fretting corrosion behavior of micro-arc oxidation coatings on zirconium alloy. Surface and Coatings Technology. 2021. V. 410. P. 126949. https://doi.org/10.1016/j.surfcoat.2021.126949

[28] Zeisig, J., Shtefan, V., Giebeler at ell. A Newly Designed High-Strength Tool Steel with High Wear and Corrosion Resistance. Materials. 2023. V. 16(5). P. 1941. https://doi.org/10.3390/ma16051941

[29] Shtefan V.V., Kanunnikova N.O., Balamut N.S. Structure and properties of chromium oxide coatings obtained by stationary and non-stationary electrolysis / Resource– and energy-saving technologies in the chemical industry : Scientific monograph. Riga, Latvia : «Baltija Publishing”, 2022, №1(11), 72-84. https://doi.org/10.30525/978-9934-26-219-7-3

Thus, in order to confirm the assumptions about the protective properties, it is necessary to conduct a study of the physicochemical properties of the formed chromoxide compositions on AISI 304 steel.

3. Physicochemical properties of chromoxide composites

The effectiveness of the use of chromoxide composites on stainless steel in various industries is evaluated as a complex of functional properties, therefore this section is devoted to the study of this complex of necessary physicochemical properties of the obtained materials[30].

***Polarization resistance*.** Voltammograms were recorded in 3% NaCl solution on an IPC-Pro potentiostat relative to a silver chloride electrode. The surface area of the working electrode was 0.5 cm^2. A potential sweep rate of 1 mV/s was started from a potential that was stable for 1 hour after immersion in the solution[31].

In fig. 7 presents for comparison the polarization dependencies of steel with a natural oxide film and with chromoxide composites obtained in a sodium chloride solution. For steel without composites and with composites, the obtained anodic and cathodic branches of the polarization dependencies are very similar to each other.

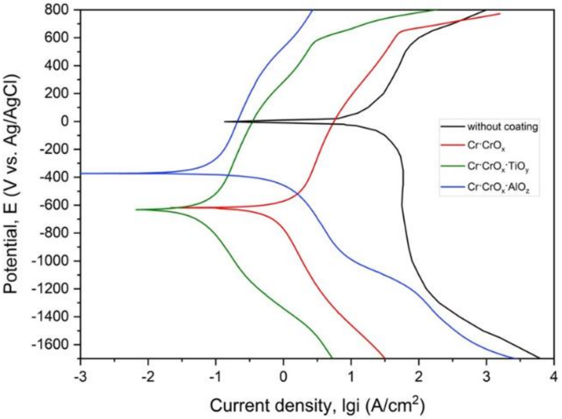

Fig. 7. Voltammograms AISI 304/without composites (1), $Cr\cdot CrO_x$, (2), $Cr\cdot CrO_x\cdot TiO_y$, (3), $Cr\cdot CrO_x\cdot Al_xO_y$ (4)

---

[30] Stern M., Geary A. L. J. Electrochem. Soc. 1957. V. 104. P. 56. https://doi.org/10.1149/1.2428496

[31] Mansfeld F. Tafel Slopes and Corrosion Rates from Polarization Resistance Measurements. Corrosion. 1973. V. 29(10). P. 397-402. https://doi.org/10.5006/0010-9312-29.10.397

According to the data of polarization studies, such corrosion characteristics as polarization resistance, Tafel steels b_k and b_a, constant B and current corrosion rate index were calculated (Table 4)[32],[33]. The addition of titanium and aluminum oxides to the composition of coatings significantly increases the polarization resistance and reduces the current corrosion rate by an order of magnitude. Thus, the chromoxide composite obtained from electrolyte No. 2 (Table 5) has the highest value of R_p, which reaches 90.2 kΩ·cm^2, which is 11.5 times more than the coating obtained from electrolyte No. 1. Thus, from the above, it can be concluded that chromoxide composites on stainless steel obtained from electrolytes No. 2 and No. 3 have more protective properties in a chloride environment.

Table 5

Corrosion characteristics of AISI 304 steel with chromoxide composites obtained in chromium-containing electrolytes with the addition of TiO_2

No.	The composition of the electrolyte, g/L	R_p, kΩ·cm^2	b_k, mV	b_a, mV	B, mV	k_j, A/m^2
Steel without composite		3,0	84	91	19	$1{,}24 \cdot 10^{-6}$
1	CrO_3 – 250, H_3BO_3 – 20, $Ba(OH)_2$ – 2, $NaNO_3$ – 5	7, 8	98	86	19	$5{,}09 \cdot 10^{-7}$
2	CrO_3 – 250, H_3BO_3 – 20, $Ba(OH)_2$ – 2, $NaNO_3$ – 5, TiO_2 – 30	68, 8	49	81	13	$3{,}87 \cdot 10^{-8}$
3	CrO_3 – 250, H_3BO_3 – 20, $Ba(OH)_2$ – 2, $NaNO_3$ – 5, TiO_2 – 50	82, 3	93	63	16	$4{,}06 \cdot 10^{-8}$
4	CrO_3 – 250, H_3BO_3 – 20, $Ba(OH)_2$ – 2, $NaNO_3$ – 5, TiO_2 – 70	87, 5	89	88	19	$4{,}42 \cdot 10^{-8}$
5	CrO_3 – 250, H_3BO_3 – 20, $Ba(OH)_2$ – 2, $NaNO_3$ – 5, TiO_2 – 100	90, 2	98	94	12	$4{,}63 \cdot 10^{-8}$

---

[32] Пат. на кор. мод. № 137165 Україна, МПК C25D 11/38. Електроліт для формування ізоляційних покриттів на нержавіючій сталі / Штефан В.В., Кануннікова Н.О., Бофанова М.В.; заявник та власник патенту НТУ «ХПІ». – № u201902705; заявл. 20.03.2019; опубл. 10.10.2019, бюл. №19. https://base.uipv.org/searchINV/search.php?action=viewdetails&IdClaim=263824

[33] Пат. на винахід № 119022 Україна, МПК C25D 11/34. Спосіб електрохімічного оксидування нержавіючої сталі / Штефан В.В., Канунікова Н.О., Баламут Н.С., Кобзєв О.В.; заявник та власник патенту НТУ «ХПІ». № a201807699; заявл. 09.07.2018; опубл. 10.04.2019, бюл. № 7. https://base.uipv.org/searchINV/search.php?action=viewdetails&IdClaim=257240

The polarization dependencies obtained on AISI 304 steel with chromoxide composites obtained from titanium-containing electrolytes (Table 5, 6) in a 3% NaCl aqueous solution indicate that due to the addition of titanium dioxide oxide layers of different concentrations to the composition, the free corrosion potential shifted to side of the electronegative value and the corrosion current decreases by an order of magnitude. Chromoxide composites obtained from electrolyte No. 3 (addition of titanium dioxide at a concentration of 30 g/L) has the lowest corrosion current.

Table 6

Corrosion characteristics of AISI 304 steel with chromoxide composites obtained in chromium-containing electrolytes with the addition of Al_2O_3

No.	**The composition of the electrolyte, g/L**	**R_p, kΩ·cm^2**	**b_k, mV**	**b_a, mV**	**B, mV**	**k_j, A/m^2**
Steel without composite		3,0	84	91	19	$1{,}24 \cdot 10^{-6}$
1	CrO_3 – 250, H_3BO_3 – 20, $Ba(OH)_2$ – 2, $NaNO_3$ – 5	7, 8	98	86	19	$5{,}09 \cdot 10^{-7}$
2	CrO_3 – 250, H_3BO_3 – 20, $Ba(OH)_2$ – 2, $NaNO_3$ – 5, Al_2O_3 – 30	45,8	76	66	15	$3{,}38 \cdot 10^{-8}$
3	CrO_3 – 250, H_3BO_3 – 20, $Ba(OH)_2$ – 2, $NaNO_3$ – 5, Al_2O_3 – 50	69, 6	63	52	12	$3{,}59 \cdot 10^{-8}$
4	CrO_3 – 250, H_3BO_3 – 20, $Ba(OH)_2$ – 2, $NaNO_3$ – 5, Al_2O_3 – 70	72,1	89	58	15	$4{,}24 \cdot 10^{-8}$
5	CrO_3 – 250, H_3BO_3 – 20, $Ba(OH)_2$ – 2, $NaNO_3$ – 5, Al_2O_3 – 100	82,3	83	90	18	$4{,}59 \cdot 10^{-8}$

As a result of polarization studies, corrosion characteristics were obtained (Table 5). On the basis of which it was established that with an increased concentration of titanium dioxide in electrolytes No. 2-5, the polarization resistance of the AISI 304/chromoxide composite system increases and the corrosion rate decreases.

Analyzing the polarization dependencies of stainless steel with chromoxide composites obtained from aluminum-containing electrolytes (Table 6)[34], it can be concluded that due to the formed oxide coating on the

---

[34] Пат. на кор. мод. № 150138 Україна, МПК C25D 11/34. Спосіб нанесення захисних хромвмісних покриттів на нержавіючу сталь / В.В. Штефан, Н.С. Баламут, Н.О. Кануннікова; заявник та патентовласник НТУ «ХПІ». – № u202104222; заяв. 19.07.2021; опубл. 05.01.2022, Бюл. №1. https://base.uipv.org/searchINV/search.php?action=viewdetails&IdClaim=280106

surface of the steel, the free corrosion potential shifted to the electronegative side and the corrosion current decreased significantly.

Impedance spectroscopy.

To study the morphology and structure of the obtained composites, the method of impedance spectroscopy in a 3% NaCl solution was used. Impedance measurements of the active R_s and capacitive component X_s were carried out in an electrochemical system, which is an IPC-Pro potentiostat and an FRA frequency response analyzer in the frequency range from 0.03 Hz to 50 kHz. The electrochemical circuit was a three-electrode system. The measurements were carried out with the polarization of the working electrode at a stationary potential, established for 1 hour. A platinum plate served as a counter electrode. A silver chloride electrode was used as a reference electrode[35].

The authors of [36] found that the impedance spectrum of the «metal-oxide-electrolyte» system is described by the equation:

$$Z = r - \frac{1}{\omega C_0} \cdot \frac{1}{1+\left(\frac{1}{\omega C_0 R_y}+tg\delta_0\right)^2} \cdot \left(\frac{1}{\omega C_0 R_y} + tg\delta_0 + j\right), \qquad (1)$$

where Z is an equivalent series resistance; ω is the frequency $(\omega=2\pi f)$; C_0 is the capacitance of the continuous oxide layer; R_y is the leakage resistance of the flaws and oxide layer conducting inclusions; r is the electrolyte layer resistance, $tg\delta_0$ is the dielectric loss angle tangent.

For the capacitance C_s and resistance R_s of the «metal-oxide-electrolyte» systems, the dependences $1/C_s \sim lgf$ and $R_s \sim 1/f$ are linear. Hence, it follows that the tangent of the dielectric loss angle $tg\delta = \omega R_s C_s$, should change very slightly with frequency, since $tg\delta = \omega R_s C_s \approx$ const, which is confirmed experimentally for tantalum [37], titanium [38], and stainless steel [39].

---

[35] Пат. на кор. мод. № 150329 Україна, МПК C01B 3/02 (2006.01), C25B 1/04 (2021.01), C25B 1/50 (2021.01). Спосіб виробництва водню електролізом / Майзеліс А.О., >Канунннікова Н.О.<. ; заявник та власник патенту НТУ «ХПІ». № u202104200; заявл. 19.07.2021; опубл. 03.02.2022, бюл. № 5. https://base.uipv.org/searchINV/search.php?action=viewdetails&IdClaim=280429

[36] Winiarski J., Cies´likowska B., Tylus W. et all. Corrosion of Nanocrystalline Nickel Coatings Electrodeposited from Choline Chloride: Ethylene Glycol Deep Eutectic Solvent Exposed in 0.05 M NaCl Solution. Appl. Surf. Sci. 2019. V 470. P. 331-339. https://doi.org/10.1016/j.apsusc.2018.11.155

[37] Cao C. Zhang J. Introduction of Electrochemical Impedance Spectroscopy; Science Press of China: Beijing, China, 2002; ISBN 7-03-009854-4.

[38] Itagaki M., Taya A., Watanabe K., Noda K. Deviations of capacitive and inductive loops in the electrochemical impedance of a dissolving iron electrode. Anal. Sci. 2002. V. 18. P. 641-644. https://doi.org/10.2116/analsci.18.641

[39] Teixeira C.H.S.B., Alvarenga E.A., Vasconcelos,W.L., Lins V.F.C. Effect of porosity of phosphate coating on corrosion resistance of galvanized and phosphated steels Part I: Measurement of porosity of phosphate. Mater. Corros. 2011. V. 62. P. 771-777. https://doi.org/10.1002/maco.200905503

According to the dependences indicated in this work, the parameters of the equivalent circuit were determined from the experimental graph of the dependence of $tg\delta$ and R_s on frequency (Figure 8) according to the formulas given in [16]:

$$tg\delta = \frac{1}{\omega C_0 R_y} + tg\delta_0 \tag{2}$$

where $tg\delta$ is the tangent of the angle of active loss.

Equivalent series resistance for composites with few defects:

$$R_s = r + \frac{1}{\omega C_0} \cdot tg\delta_0, \tag{3}$$

where r is the resistance of the electrolyte layer between the electrodes.

In the graph and in the table, instead of the angular frequency ω, the frequencies f are indicated in *Hz*[40].

The graph of $tg\delta$ versus frequency shown in Figure 8 fully corresponds to equation (1). The position of the tgδ minimum and the change in the slopes of the curves depend on the resistance of the electrolyte, as follows from equation (1). It is obvious that the presence of aluminum and titanium compounds in the composites changes the slope of the $tg\delta$ dependence on frequency in the frequency range from 50 to 200 Hz.

The dependences of the impedance parameters of the «metal-oxide-electrolyte» system on the composition of the composites are presented in Table 5. The composites formed in electrolytes containing titanium and aluminum have pores and defects to a lesser extent than the composites formed in the main electrolyte, as evidenced by an increase in the $tg\delta_0$ value.

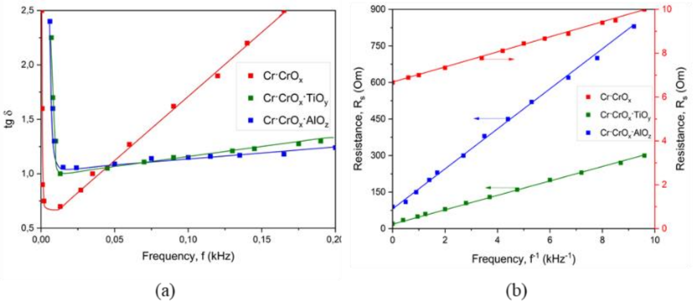

(a) (b)

Fig. 8. Frequency dependence of $tg\delta$ (a) and equivalent series resistance R_s(b) of the steel/composites: $Cr\cdot CrO_x$ (1), $Cr\cdot CrO_x\cdot TiO_y$ (2), $Cr\cdot CrO_x\cdot Al_xO_y$ (3)

---

[40] Cottis, R.; Turgoose, S. Electrochemical Impedance and Noise; Syrett, B.C., Ed.; NACE International: Houston, TX, USA, 1999; ISBN 157-590-0939.

Table 5

The relationship of the parameters of «steel-oxide– electrolyte» system as a function of the chromoxide composites composition in 3% NaCl

Parameters	**Chromxide composites**		
	$Cr\cdot CrO_x$	**$Cr\cdot CrO_x\cdot TiO_y$**	**$Cr\cdot CrO_x\cdot Al_xO_y$**
r, kΩ·cm^2	6,6	29,9	88,4
R_y, kΩ·cm^2	1,5	163,9	730,9
C_0, μF	269,6	5,3	1,8
f_{min}, Hz	12,4	26,0	16,0
$tg\delta_0$	0,568	0,967	0,951

From Table 5 that the presence of titanium compounds in the composition of composites, and especially aluminum, leads to a significant increase in the value of R_y, which determines the conductivity based on oxide film defects. This fact indicates a decrease in the defectiveness of titanium– and aluminum-containing composites in relation to the composites obtained from the base electrolyte.

Electrical insulation. To measure the electrical resistance of the insulation of the composites, an E6-13 teraometer was used with a three-electrode system, which consisted of measuring, high-voltage guard electrode. The samples were rectangular 5 mm in size. The diameter of the guard electrode was 74 mm, and the diameter of the high-voltage electrode was slightly larger, since there are oxide films on the samples. The measuring electrode was pressed against the test sample with a certain force. The gap between the measuring electrode and the inner diameter of the guard electrode was q = 2 mm. The tests were carried out at 18-25°C[41].

The composites obtained on the surface of stainless steel lead to a sharp increase in the electrical resistance of insulation (R_{ins}), so for steel made of $Cr\cdot CrO_x$ it was $0{,}61\cdot 106$ kΩ·cm^2, for steel made of $Cr\cdot CrO_x\cdot TiO_y$ $9{,}00\cdot 10^9$ kΩ·cm^2, and for steel from $Cr\cdot CrO_x\cdot Al_xO_y$ $2{,}10\cdot 10^7$ kΩ·cm^2.

Consequently, the resulting composites exhibit high electrical insulation properties. Steel with $Cr\cdot CrO_x\cdot TiO_y$ composites has the highest value of R_{ins}. Thus, composites on AISI 304 steel can be offered as electrical insulating materials for various industries.

CONCLUSIONS

The determined kinetic regularities of the cathodic formation of composites from chromium-containing electrolytes with the addition of titanium and aluminum oxides indicate a change in the mechanism of cathodic hydrogen release with an increase in the concentration of the added oxides. It

---

[41] Bejinariu C., Burduhos-Nergis D.P., Cimpoesu N., Bernevig-Sava M.A. et all. Study on the anticorrosive phosphated steel carabiners used at personal protective. Calitatea. 2019. V. 20. P. 71.

was determined that an increase in the concentration of titanium or aluminum oxides in chromium-containing electrolytes during the cathodic formation of chromoxide composites causes a change in the limiting stage of the electrochemical process.

It was established that aluminum and titanium oxides increase the integrity and reduce the width of cracks on chromoxide composites. EDX – surface spectra confirmed the presence of aluminum and titanium compounds in the composites.

The results of polarization studies proved that the addition of aluminum and titanium oxides to the composition of composites increases the polarization resistance and reduces the corrosion rate of steel with chromoxide composites in a chloride environment.

To study the properties of the obtained composites, the method of impedance spectroscopy was used. It was found that the presence of titanium and aluminum compounds in the chromoxide composites leads to a decrease in the conductivity of the composites. It was found that the presence of titanium and aluminum oxides in the composition of composites increases the value of R_s by 34-497 times, which indicates a decrease in defectively and electrical conductivity of chromoxide composites. Based on certain electrochemical parameters, it was found that the protective effect of the composite is due to a decrease in the electrical conductivity of the composites due to the introduction of titanium and aluminum oxides.

SUMMARY

The determination of the kinetic regularities of the cathodic formation of chromoxide composites on steel in chromium-containing electrolytes containing aluminum or titanium oxides is presented. The morphology, elemental and phase compositions of the obtained chromoxide composites were studied. Corrosion characteristics such as polarization resistance, Tafel steels b_k and b_a, constant B and current corrosion rate index were calculated, which indicate high protective properties of composites. It has been proven that the presence of aluminum and titanium oxides in chromoxide composites leads to a decrease in the conductivity of the coatings and defectiveness of the materials. It has been found that when the composites are modified with titanium and aluminum oxides, the electrical resistance of the composites insulation increases.

Bibliography

1. Haq I.U., Akhtar K., Khan Tahir.I., Ali Shah A. Electrodeposition of Ni–Fe_2O_3 nanocomposite coating on steel. *Surface and Coatings Technology*. 2013. V. 235. P. 691-698. https://doi.org/10.1016/j.surfcoat.2013.08.048.

2. Georgieva J., Armyanov S., Valova E., Poulios I., Sotiropoulos S. Preparation and photoelectrochemical characterisation of electrosynthesised titanium dioxide deposits on stainless steel substrates. *Electrochimica Acta*. 2006. V. 51. P. 2076-2087. https://doi.org/10.1016/j.electacta.2005.07.017.

3. Junqueira R.M.R., Manfridini A.P. de Andrade, Loureiro C.R. de Oliveira et all. Morphological, chemical and mechanical characteristics of an anodic coating on stainless steel. *Surface Engineering*. 2013. V. 29. P. 379-383. https://doi.org/10.1179/1743294413Y.0000000126.

4. Klimas V., Pakštas V., Vrublevsky I., Chernyakova K., Jagminas A. Fabrication and Characterization of Anodic Films onto the Type-304 Stainless Steel in Glycerol Electrolyte. *J. Phys. Chem. C*. 2013. V. 117. P. 20730-20737. https://doi.org/10.1021/jp407028u.

5. Arevalo Marulanda J.L., Pérez Trujillo F.J., Castañeda S.I. Aluminum-silicon coatings on austenitic stainless steel (AISI 304 and 317) deposited by chemical vapor deposition in a fluidized bed: Recubrimientos de aluminio-silicio sobre acero inoxidable austenítico AISI 304 Y 317 por deposición química de vapor en lecho fluidizado. *Ing. Inv*. 2014. V. 34. P. 5-10. https://doi.org/10.15446/ing.investig.v34n2.41249.

6. Shtefan V.V., Smyrnov O.O., Bezhenko A.O., Epifanova A.S., Kanunnikova N.O., Metenkanych M.M., Knyazev S.A. Corrosion of Cobalt-Molybdenum Alloys in Chloride Solutions. *Mater Sci*. 2019. V. 54 P. 512-518. https://doi.org/10.1007/s11003-019-00225-y.

7. Ingle A.V., Raja V.S., Mishra P. et al, Effect of Mo Addition on the Corrosion Behavior of Al-40Cr-xMo Coatings on Type 316L Stainless Steel. *Metall Mater Trans A*. 2020. V. 51. P. 1933-1944. https://doi.org/10.1007/s11661-020-05628-0.

8. Bellezze T., Roventi G., Quaranta A., Fratesi R. Improvement of pitting corrosion resistance of AISI 444 stainless steel to make it a possible substitute for AISI 304L and 316L in hot natural waters: Improvement of pitting corrosion resistance of stainless steel. *Materials and Corrosion*. 2008. V. 59. P. 727-731. https://doi.org/10.1002/maco.200804112.

9. Shen Y.Z., Guo X.Z., Lin Y.BTao., J. Al_2O_3 coatings fabricated on stainless steel/aluminium composites by microarc oxidation. *Surface Engineering*. 2014. V. 30. P. 735-740. https://doi.org/10.1179/1743294414Y.0000000300.

10. Šípová M., Marušáková D., Aparicio C., Procházka J., Halodová P. A study on the corrosion behaviour of stainless steel 08Cr18Ni10Ti in supercritical water. Corrosion Science. 2023.Vol. 211. P. 110853. https://doi.org/10.1016/j.corsci.2022.110853.

11. Rajakaruna R. M. P. I., Ariyarathna, I. R. Functionalized metal-based nanoelectrocatalysts for water splitting. *Handbook of Functionalized*

Nanomaterials for Industrial Applications. 2020. P. 83–109. https://doi.org/10.1016/b978-0-12-816787-8.00004-1.

12. Huang L., Yao B., Sun J. et all. Highly conductive and flexible molybdenum oxide nanopaper for high volumetric supercapacitor electrode. *J. Mater. Chem. A.* 2017. V. 5. P. 2897-2903. https://doi.org/10.1039/C6TA10433A.

13. Shtefan V.V., Kanunnikova N.O., Goncharenko T.Ye. Analysis of the Structure and Anticorrosion Properties of Oxide Coatings on AISI 304 Steel. *Mater Sci.* 2021. V. 57. P. 248-255. https://doi.org/10.1007/s11003-021-00539-w.

14. Geng S., Qi S., Zhao Q., Zhu S., Wang F. Electroplated Ni–Fe_2O_3 composite coating for solid oxide fuel cell interconnect application. *International Journal of Hydrogen Energy*. 2012. V. 37. P. 10850-10856. https://doi.org/10.1016/j.ijhydene.2012.04.043.

15. Shtefan V.V., Balamut N.S., Kanunnikova N.A. et all. Electrodeposition of chromoxide coatings from electrolytes modified with $SiO_2 \cdot nH_2O$, *Problems of Atomic Science and Technology(PAST),* 2022. V. 140. P. 131-136. https://doi.org/10.46813/2022-140-131.

16. Taveira L.V., Montemor M.F., Belo M. Da Cunha. Influence of incorporated Mo and Nb on the Mott–Schottky behaviour of anodic films formed on AISI 304L. *Corrosion Science*. 2010. V. 52. P. 2813-2818. https://doi.org/10.1016/j.corsci.2010.04.021.

17. Shtefan V., Kanunnikova N., Balamut N. Anodic oxidation of AISI 304 steel in acidic solutions. *Proceedings of Odessa Polytechnic University.* 2018. V 56. № 3. P. 89-94. https://doi.org/10.15276/opu.3.56.2018.09.

18. Maier B., Frankel G. S. Pitting Corrosion of Bare Stainless Steel 304 under Chloride Solution Droplets. *Journal of The Electrochemical Society*. 2010. V. 157(10). P. 302. https://doi.org/10.1149/1.3467850.

19. Shtefan V., Kanunnikova N., Bulhakova A. et al. Structural and Phase Analysis of Composites Based on TiO_2. *Surf. Engin. Appl.Electrochem*. V. 58. P. 598-603 https://doi.org/10.3103/S1068375522060138.

20. Пат. на кор. мод. № 147835 Україна, МПК C25D 11/34. Спосіб формування захисних оксидних покриттів на нержавіючій сталі / Штефан В.В., Смирнова О.Ю., Кануннікова Н.О. Баламут Н.С.; заявник та власник патенту НТУ «ХПІ». – № u202008156; заявл. 21.12.2020; опубл. 16.06.2021, бюл. № 24.

https://base.uipv.org/searchINV/search.php?action=viewdetails&IdClaim=276584.

21. Zuyok V., Rud R., Shtefan V. et all. Assessment of the corrosion resistance of the main alternative materials for light water reactors tolerant

fuel rod cladding. *Problems of Atomic Science and Technology*. 2022. V. 140(4). P. 89-96. https://doi.org/10.46813/2022-140-089.

22. Mansfeld F., Kendig, M. Technical Note:Concerning the Choice of Scan Rate in Polarization Measurements. *Corrosion*. 1981. V. 37(9). P. 545-546. https://doi.org/10.5006/1.3580804.

23. Shtefan V.V., Kanunnikova N.A. Oxidation of AISI 304 Steel in Al– and Ti-Containing Solutions. *Prot Met Phys Chem Surf*. 2020. V. 56. P. 379-384. https://doi.org/10.1134/S2070205120020239.

24. Shtefan V.V., Kanunnikova N.O., Balamut N.S. Structure and properties of chromium oxide coatings obtained by stationary and non-stationary electrolysis / Resource– and energy-saving technologies in the chemical industry : Scientific monograph. Riga, Latvia : «Baltija Publishing», 2022, №1(11), 72-84. https://doi.org/10.30525/978-9934-26-219-7-3.

25. Slemnik M., Milošev I. An impedance study of two types of stainless steel in Ringer physiological solution containing complexing agents. *Journal of Materials Science: Materials in Medicine*. 2006. V. 17(10). P. 911-918. https://doi.org/10.1007/s10856-006-0180-0.

26. Shtefan V.V., Kanunnikova N.A. Electrochemical formation of molybdenum-coating anode oxide coatings on AISI 304 steel. *Promising Materials and Processes in Applied Electrochemistry*: Monograph / Editor-in-chief V.S. Barsukov. Kyiv: KNUTD. 2019. P. 97-110.

27. Li Z.Y., Cai Z.B., Cui X.J. et al., Influence of nanoparticle additions on structure and fretting corrosion behavior of micro-arc oxidation coatings on zirconium alloy. *Surface and Coatings Technology*. 2021. V. 410. P. 126949. https://doi.org/10.1016/j.surfcoat.2021.126949.

28. Shtefan V., Kanunnikova N., Pilipenko A., Pancheva H. Corrosion Behavior of AISI 304 Steel in Acid Solutions. *Materials Today: Proceedings*. 2019. V. 6. P. 150-157. https://doi.org/10.1016/j.matpr.2018.10.088.

29. Zeisig, J., Shtefan, V., Giebeler at ell. A Newly Designed High-Strength Tool Steel with High Wear and Corrosion Resistance. *Materials*. 2023. V. 16(5). P. 1941. https://doi.org/10.3390/ma16051941.

30. Stern M., Geary A. L. *J. Electrochem. Soc*. 1957. V. 104. P. 56. https://doi.org/10.1149/1.2428496.

31. Mansfeld F. Tafel Slopes and Corrosion Rates from Polarization Resistance Measurements. *Corrosion*. 1973. V. 29(10). P. 397-402. https://doi.org/10.5006/0010-9312-29.10.397.

32. Пат. на кор. мод. № 137165 Україна, МПК C25D 11/38. Електроліт для формування ізоляційних покриттів на нержавіючій сталі / Штефан В.В., Кануннікова Н.О., Бофанова М.В.; заявник та власник патенту НТУ «ХПІ». – № u201902705; заявл. 20.03.2019; опубл. 10.10.2019, бюл. № 19.

https://base.uipv.org/searchINV/search.php?action=viewdetails&IdClaim=263824.

33. Пат. на винахід № 119022 Україна, МПК C25D 11/34. Спосіб електрохімічного оксидування нержавіючої сталі / Штефан В.В., Кануннікова Н.О., Баламут Н.С., Кобзєв О.В.; заявник та власник патенту НТУ «ХПІ». № a201807699; заявл. 09.07.2018; опубл. 10.04.2019, бюл. № 7. https://base.uipv.org/searchINV/search.php?action=viewdetails&IdClaim=257240.

34. Пат. на кор. мод. № 150138 Україна, МПК C25D 11/34. Спосіб нанесення захисних хромвмісних покриттів на нержавіючу сталь / В.В. Штефан, Н.С. Баламут, Н.О Кануннікова; заявник та патентовласник НТУ «ХПІ». – № u202104222; заяв. 19.07.2021; опубл. 05.01.2022, Бюл. № 1. https://base.uipv.org/searchINV/search.php?action=viewdetails&IdClaim=280106.

35. Пат. на кор. мод. № 150329 Україна, МПК C01B 3/02 (2006.01), C25B 1/04 (2021.01), C25B 1/50 (2021.01). Спосіб виробництва водню електролізом / Майзеліс А.О., >Канунннікова Н.О.<. ; заявник та власник патенту НТУ «ХПІ». № u202104200; заявл. 19.07.2021; опубл. 03.02.2022, бюл. № 5. https://base.uipv.org/searchINV/search.php?action=viewdetails&IdClaim=280429.

36. Winiarski J., Cies´likowska B., Tylus W. et all. Corrosion of Nanocrystalline Nickel Coatings Electrodeposited from Choline Chloride: Ethylene Glycol Deep Eutectic Solvent Exposed in 0.05 M NaCl Solution. *Appl. Surf. Sci*. 2019. V 470. P. 331-339. https://doi.org/10.1016/j.apsusc.2018.11.155.

37. Cao C. Zhang J. Introduction of Electrochemical Impedance Spectroscopy; Science Press of China: Beijing, China, 2002; ISBN 7-03-009854-4.

38. Itagaki M., Taya A., Watanabe K., Noda K. Deviations of capacitive and inductive loops in the electrochemical impedance of a dissolving iron electrode. *Anal. Sci*. 2002. V. 18. P. 641-644. https://doi.org/10.2116/analsci.18.641.

39. Teixeira C.H.S.B., Alvarenga E.A., Vasconcelos,W.L., Lins V.F.C. Effect of porosity of phosphate coating on corrosion resistance of galvanized and phosphated steels Part I: Measurement of porosity of phosphate. *Mater. Corros*. 2011. V. 62. P. 771-777. https://doi.org/10.1002/maco.200905503.

40. Cottis, R.; Turgoose, S. Electrochemical Impedance and Noise; Syrett, B.C., Ed.; NACE International: Houston, TX, USA, 1999; ISBN 157-590-0939.

41. Bejinariu C., Burduhos-Nergis D.P., Cimpoesu N., Bernevig-Sava M.A. et all. Study on the anticorrosive phosphated steel carabiners used at personal protective. *Calitatea.* 2019. V. 20. P. 71.

Information about the authors:
Shtefan Viktoriia Volodymyrivna,
Doctor of Technical Sciences,
Professor at the Department of Technical Electrochemistry
National Technical University «Kharkiv Polytechnic Institute»
2, Kyrpychova str., Kharkiv, 61002, Ukraine

Kanunnikova Nadiia Oleksandrivna,
Doctor of Philosophy,
Research Fellow at the Department of Technical Electrochemistry
National Technical University «Kharkiv Polytechnic Institute»
2, Kyrpychova str., Kharkiv, 61002, Ukraine

Dubrovskyi Vladyslav Stanislavovych,
Student at the Department of Technical Electrochemistry
National Technical University «Kharkiv Polytechnic Institute»
2, Kyrpychova str., Kharkiv, 61002, Ukraine